Hyperbolic heat conduction restricted by continuous boundary interface*

JIANG Fangming (蒋方明) and LIU Dengying (刘登瀛)

Institute of Engineering Thermophysics, Chinese Academy of Sciences, Beijing 100080, China

Received April 27, 2000; revised September 29, 2000

Abstract Finite difference method (FDM) combined with MacCormack's predictor-corrector scheme is used to solve the problem of hyperbolic heat conduction in a finite medium. One of its boundary surfaces is heated by a rectangular pulsed energy source while the other surface is tightly contacted with another medium where the continuous boundary condition is satisfied. Some non-Fourier heat conduction behaviors have been analyzed theoretically.

Keywords: hyperbolic heat conduction (HHC), non-Fourier heat conduction, MacCormack's predictor-corrector scheme.

The non-Fourier heat conduction phenomenon observed in many media[1~3] has potential uses in many engineering processes, such as rapid melting and solidifying of metal, surface heat treatment with laser, temperature controlling of superconductors, handling of the accident of nuclear device, laser surgery in biomedical engineering and impulse drying. There is still much work to do before we make use of the non-Fourier heat conduction in engineering areas.

In this paper, the hyperbolic heat conduction (HHC) model is chosen to analyze one special non-Fourier heat conduction case, in which one of the boundary surfaces of a finite medium is heated by a rectangular pulsed energy source and the other boundary is tightly contacted with another medium where the continuous boundary condition (the fourth kind of heat transfer boundary condition) is satisfied.

Some theoretical analyses[4, 5] and experimental studies[1] of non-Fourier heat conduction indicate that the evident non-Fourier heat conduction behavior can only exist in a very thin layer of the medium and the heat transfer in the other part of the medium still complies with the Fourier law perfectly. In the interface of those two parts, the 4th kind of boundary condition should be satisfied. Therefore the problem studied in this paper is relevant to practical engineering and the result will have great application values. Obviously, it is difficult to obtain an analytical solution of this kind of non-Fourier heat conduction problem because of its extreme complexity. Numerical solution with finite difference method (FDM) will be found out for the numerical difference of the hyperbolic heat conduction equation, where the MacCormack's predictor-corrector scheme[6] is used to deal with the numerical formulation. The results will reveal some non-Fourier heat conduction behaviors in the medium.

* Project supported by the Chinese Academy of Sciences (Grant No. KJ 951-B1-704), the National Natural Science Foundation of China (Grant No. 59736130) and the National Key Basic Research Science Foundation (Grant No. G20000, 26305).

1 Formulation

1.1 1-D physical model

A finite medium, $0 \leqslant x_s \leqslant \delta$, is placed on a large base, $0 \leqslant x_b \leqslant l$ (Fig. 1). Both the finite medium and the base are initially at temperature $T_{s(x_s,0)} = T_{b(x_b,0)} = T_0$(the room temperature). For time $t > 0$, the boundary surface at $x_s = 0$ is heated by a rectangular pulsed energy source and the boundary surface, $x_s = \delta$, is tightly contacted with the base's boundary surface, $x_b = 0$, where the 4th kind of boundary condition is satisfied, while the other boundary surface of the base, $x_b = l$, is kept insulated.

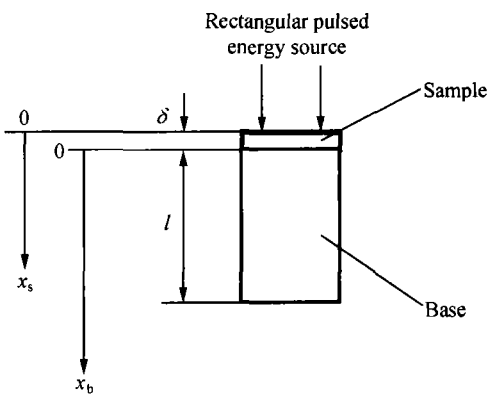

Fig. 1 Computational model.

1.2 Governing equations

The heat transfer in the sample (finite medium) is considered as the non-Fourier heat conduction and the hyperbolic heat conduction model is employed to describe it, while the heat transfer in the base is still governed by the Fourier law and the classical parabolic heat conduction model is used. The governing equations including the initial and boundary conditions can be obtained as follows.

1.2.1 For the sample. The governing equations for heat transfer in the sample can be expressed as

$$\tau \frac{\partial q_{s(x_s,t)}}{\partial t} + q_{s(x_s,t)} = -\lambda_s \frac{\partial T_{s(x_s,t)}}{\partial x_s}, \quad (0 < x_s < \delta), \tag{1}$$

$$\frac{\partial q_{s(x_s,t)}}{\partial x_s} = -(\rho c_p)_s \frac{\partial T_{s(x_s,t)}}{\partial t}, \quad (0 < x_s < \delta), \tag{2}$$

where the thermal relaxation time τ (or thermal characteristic time for porous material) is defined as $\tau = \frac{a_s}{c^2}$. a_s is the thermal diffusivity of the sample and c the velocity of the propagation of thermal disturbance in the sample.

The initial conditions are

$$T_{s(x_s,0)} = T_0, \quad (0 \leqslant x_s \leqslant \delta), \tag{3}$$

$$q_{s(x_s,0)} = 0, \quad (0 \leqslant x_s \leqslant \delta). \tag{4}$$

It is necessary to describe two boundary conditions at the interface of the sample and the base because both the temperature and the heat flux at the interface are unknown. The continuities of temperature and heat flux at the interface must be employed together. So the boundary conditions are

$$q_{s(0,\,t)} = q_0 \cdot U_{(t)}, \tag{5}$$

$$q_{s(\delta,\,t)} = q_{b(0,\,t)}, \tag{6}$$

$$T_{s(\delta,\,t)} = T_{b(0,\,t)}. \tag{7}$$

In Eq. (5), q_0 is the heat flux density of the rectangular pulsed energy source and the $U_{(t)}$ denotes a unit pulsed function and can be expressed as

$$U_{(t)} = \begin{cases} 0 & t < 0, \\ 1 & 0 \leqslant t \leqslant t_p, \\ 0 & t > t_p, \end{cases}$$

where t_p is the pulse duration of the rectangular pulsed energy source.

1.2.2 For the base. The heat transfer in the base is governed by the Fourier law and the governing equations can be written as

$$q_{b(x_b,\,t)} = -\lambda_b \frac{\partial T_{b(x_b,\,t)}}{\partial x_b}, \quad (0 < x_b < l), \tag{8}$$

$$\frac{\partial q_{b(x_b,\,t)}}{\partial x_b} = -(\rho c_p)_b \frac{\partial T_{b(x_b,\,t)}}{\partial t}, \quad (0 < x_b < l). \tag{9}$$

Initial conditions are

$$T_{b(x_b,\,0)} = T_0, \quad (0 \leqslant x_b \leqslant l), \tag{10}$$

$$q_{b(x_b,\,0)} = 0, \quad (0 \leqslant x_b \leqslant l), \tag{11}$$

and the boundary conditions are

$$q_{b(0,\,t)} = q_{s(\delta,\,t)}, \tag{6}'$$

$$T_{b(0,\,t)} = T_{s(\delta,\,t)}, \tag{7}'$$

$$q_{b(l,\,t)} = 0. \tag{12}$$

1.3 Numerical analysis

Finite difference method (FDM) is used to numerically analyze the aforementioned thermal case. The numerical treatment of Eqs. (1) ~ (12) is routine, so it is omitted here.

The network of grid points of the sample and the base is shown in Fig. 2. For this sample, there are $M + 1$ (from 0 to M) nodal points for the temperature T_s and $M + 2$ (from 0 to $M + 1$) nodal points for the heat flux density q_s. The base has $N + 1$ (from 0 to N) nodal points for its temperature T_b and $N + 2$ nodal points for its heat flux density q_b.

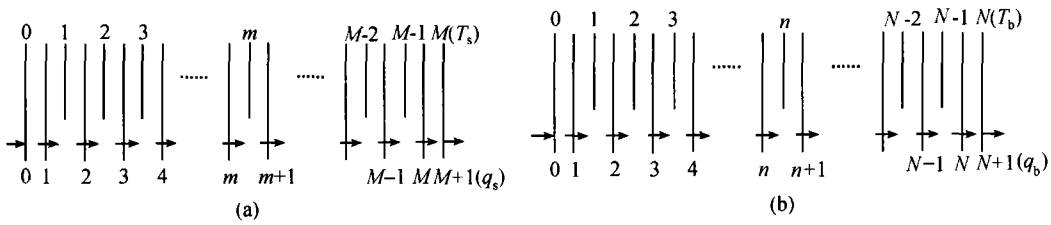

Fig. 2 Network of grid points for numerical analysis of the sample and the base. (a) For the sample; (b) for the base.

1.4 MacCormack's P-C method

In order to handle the sharp discontinuities at the wave front with high resolution and small oscillation, the MacCormack's predictor-corrector scheme[6] is used to improve the obtained numerical equations in subsec. 1.3. The MacCormack's predictor-corrector method can be illustrated with the following example.

If a numerical formulation is expressed as $F^{i+1} = H^i$, then the predictor is formulated as $\tilde{F}^{i+1} = H^i$ and the corrector can be written as $F^{i+1} = (F^i + \tilde{H}^{i+1})/2$.

For example, the numerical form of Eq. (1) is

$$q_{s,m}^{i+1} = q_{s,m}^{i} - \Delta t \frac{q_{s,m}^{i}}{\tau} - \lambda_s \frac{T_{s,m}^{i} - T_{s,m-1}^{i}}{\Delta x_s} \cdot \frac{\Delta t}{\tau}, \quad m \in [1, M]. \tag{13}$$

Here the grid points are identified with m and i, m being the number of x_s-increments and i the number of time t-increments.

Its predictor and corrector can be expressed as follows.

The predictor is

$$\tilde{q}_{s,m}^{i+1} = q_{s,m}^{i} - \Delta t \frac{q_{s,m}^{i}}{\tau} - \lambda_s \frac{T_{s,m}^{i} - T_{s,m-1}^{i}}{\Delta x_s} \cdot \frac{\Delta t}{\tau}, \tag{14}$$

and the corrector is

$$q_{s,m}^{i+1} = \left(q_{s,m}^{i} + \tilde{q}_{s,m}^{i} - \Delta t \frac{\tilde{q}_{s,m}^{i}}{\tau} - \lambda_s \frac{\tilde{T}_{s,m}^{i} - \tilde{T}_{s,m-1}^{i}}{\Delta x_s} \cdot \frac{\Delta t}{\tau} \right)/2. \tag{15}$$

After the predictor and corrector expressions of all numerical formulations have been obtained, the iteration process can be started and the temperature variation at any position of the sample can be obtained.

2 Results and discussions

With the non-Fourier heat conduction behavior in the sample in mind, attention is p aid to the temperature variation at the interface. The effects of the parameters λ_b/λ_s, $(\rho c_p)_b/(\rho c_p)_s$, τ, t_p, q_0 and x_s on the temperature variation are carefully examined. The parameters needed in numerical computation are shown in Table 1.

Table 1 Assumed parameters in computational process

		δ /μm	l /mm	λ_s/W·m^{-1}·K^{-1}	λ_b/W·m^{-1}·K^{-1}	$(\rho c_p)_s$ /kJ·m^{-3}·K^{-1}	$(\rho c_p)_b$ /kJ·m^{-3}·K^{-1}	τ /μs	q_0 MW·m^{-2}	t_p/ μs	T_0 /K	M	N	Δt/μs
Fig. 3	(a)	25	24	100	120	2000	2500	5	20	5	20	10	30	0.00003
	(b)	25	24	100	100	2000	2000	10	20	5	20	10	30	0.00003
Fig. 4		25	24	100	120	2000	2500	–	20	5	20	10	30	0.00003
Fig. 5	(a)	25	24	100	–[a]	2000	2500	10	20	5	20	10	30	0.00003
	(b)	25	24	100	120	2000	–[a]	10	20	5	20	10	30	0.00003
Fig. 6	(a)	25	24	100	120	2000	2500	5	–[a]	5	20	10	30	0.00003
	(b)	25	24	100	120	2000	2500	5	–[a]	–[a]	20	10	30	0.00003

a) The value of the parameter can be found out in the corresponding paper.

Figure 3(a) shows the temperature variation at different positions ($x_s = 0$, $x_s = \delta/2$, $x_s = \delta$) in the sample. It can be easily discovered that the thermal propagation in the sample, predicted by the HHC model, deviates evidently from the classical thermal diffusion and shows some wave nature. With increasing x_s, the varying amplitude of temperature attenuates. The maximum temperature change in the medium is much larger than that predicted by the Fourier law. During some time period and at certain position in the sample, the temperature may be higher than that of the heated surface ($x_s = 0$). For example, during 17 ~ 19 microseconds in Fig. 3(a) the temperature at $x_s = \delta/2$ is higher than that at $x_s = 0$. The temperature variation shows typical non-Fourier heat conduction behavior.

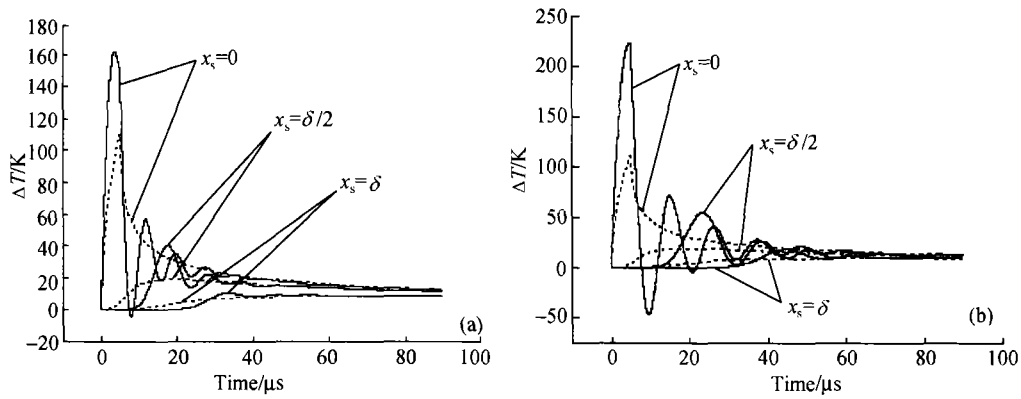

Fig. 3 Temperature variation in the sample. (a) The sample and the base have different thermal properties; (b) the sample and the base have uniform thermal properties. —, HHC; - - - PHC.

Figure 3(b) shows a very special and interesting case. The thermal properties (heat conductivity and volumetric heat capacity) of the sample and the base are uniform, i.e. they are the same kind of material. The interface between them is just imaginary. Non-Fourier heat conduction behavior in the sample is still very evident. This case may be very common in practical engineering because the non-Fourier heat conduction behavior can only exist in a very thin layer near the thermal disturbance and it is unlikely to influence the whole macroscopic object. For this case the method used here is effective. We might define the area where the non-Fourier heat conduction prevails as "the thin layer of non-Fourier heat conduction". The thickness of this layer is very important in the practical application of non-Fourier heat conduction. It is worthwhile to further study this problem in the future.

The effect of τ on the temperature variation in the interface is shown in Fig. 4. The larger the τ is, the more significant the non-Fourier heat conduction in the sample will be. When τ equals 2 μs,

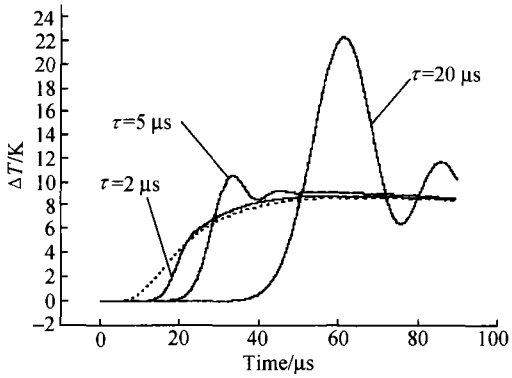

Fig. 4 Effect of τ on the temperature of the interface. ——, HHC, ·····, PHC.

the temperature variation in the interface is nearly comparable with that computed by the PHC model. This indicates that τ is an important factor to determine whether the non-Fourier heat conduction behaviors are significant or not.

The thermal properties of the base also have significant influences on the temperature of the sample. Fig. 5(a) and (b) show the effects of λ_b/λ_s and $(\rho c_p)_b/(\rho c_p)_s$ on the temperature of the interface, respectively. The larger either one of the two ratios is, the weaker the non-Fourier heat conduction behavior is. This result suggests that if a weaker non-Fourier heat conduction behavior is expected for the sample, a base that has a larger heat conductivity and heat capacity should be put under the sample.

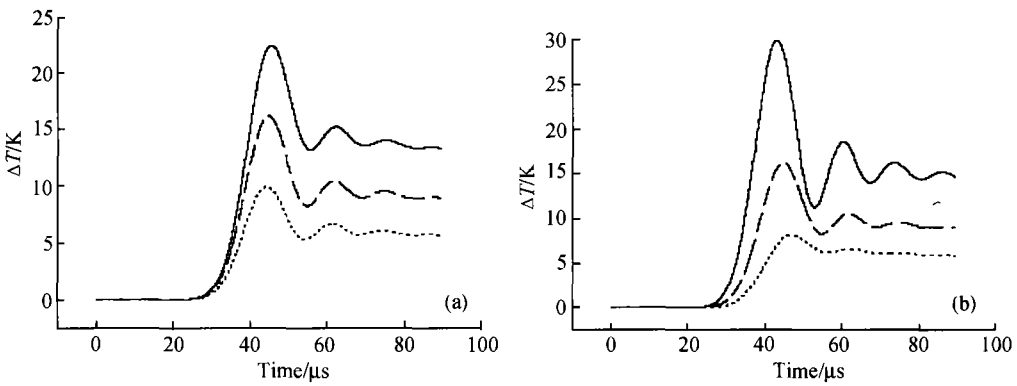

Fig. 5 Influences of the thermal properties of the base on the temperature of the interface. (a) Effect of λ_b/λ_s; (b) effect of $(\rho c_p)_b/(\rho c_p)_s$. In (a) —, $\lambda_b/\lambda_s=0.2$; - - -, $\lambda_b/\lambda_s=1.2$; ------, $\lambda_b/\lambda_s=5$. In (b) $(\rho c_p)_s/\rho c_p)_s=0.1$; - - -, $(\rho c_p)_b(\rho c_p)_s=1.25$; ------, $(\rho c_p)_s/(\rho c_p)_s=5$.

The effect of the intensity q_0 of the rectangular pulsed energy source on the non-Fourier heat conduction behavior is shown in Fig. 6(a). With an increase in the pulsed energy source's intensity, the fluctuation amplitude of the temperature becomes greater.

The pulse duration t_p of the pulsed energy source reflects the instantaneity of the thermal disturbance. Generally speaking, the shorter the t_p is, the stronger the instantaneity of the pulsed energy source will be and the non-Fourier heat conduction behavior in the sample will be more evident. Fig. 6(b) testifies this point. It can be discovered from Fig. 6(b) that when t_p equals 50 microseconds, the temperature variation of the interface shows little deviation from that predicted by the PHC model.

3 Conclusions

In this paper, non-Fourier hyperbolic heat conduction in a finite medium restricted by the 4th kind of boundary condition is numerically solved with the FDM combined with the MacCormack's predictor-corrector method. The non-Fourier heat conduction behaviors in the sample are carefully stud-

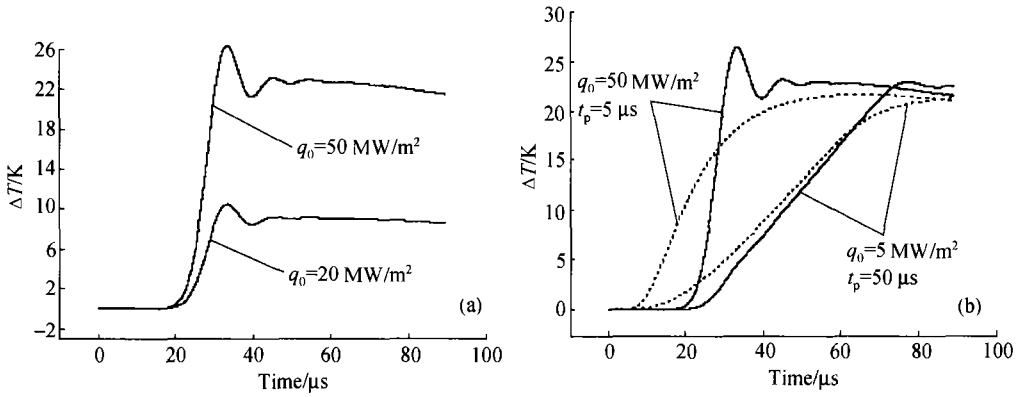

Fig. 6 Influences of the parameters of thermal disturbance on the temperature of the interface. (a) Effect of q_0; (b) effect of t_p. —, HHC; - - -, PHC.

ied. The results show that the smaller x_s, λ_b/λ_s, $(\rho c_p)_b/(\rho c_p)_s$ are, the shorter τ, t_p are, and the greater q_0 is, the stronger the non-Fourier heat conduction behaviors are. Conclusions can be drawn as follows.

(i) In practical engineering, the heated material is given, i.e. τ, λ and ρc_p are all constant, the non-Fourier heat conduction behavior in the material can be controlled by controlling q_0 and t_p. For example, in some laser surgeries, a stronger non-Fourier effect is expected, so a laser pulse with short duration and high intensity can be chosen as the heating source. On the other hand, in some surface heat treatments, a weaker non-Fourier effect is expected, so a weaker laser pulse with long duration or a continuous laser beam is the most suitable choice.

(ii) A temperature control method is suggested based on the relation of the non-Fourier heat conduction behavior in the sample and the base's thermal properties. For example, if some weaker non-Fourier heat conduction is expected in the sample, a base that has a greater heat conductivity and volumetric heat capacity can be put under it.

(iii) The physical model discussed in this paper has a wide application in practical engineering.

(iv) The non-Fourier temperature variation obtained in this paper is similar to the experimental result reported in Ref. [1] qualitatively.

References

1 Liu, D. et al. Experimental study on non-Fourier heat conduction in several kinds of porous material. In: 1st International Conference on Engineering Thermophysics (ICET), Beijing, August 18 ~ 21, 1999.
2 Peshkov, V. Second sound in helium II. Journal of Physics, USSR, 1944, 8: 381.
3 Qiu, T. et al. Femtosecond laser heating of multi-layer metals——II. Experiments. Int. J. Heat Mass Transfer, 1994, 37(17): 2799.
4 Cai, R. et al. One-dimensional algebraic explicit analytical solution of unsteady non-Fourier heat conduction in a sphere. Progress in Natural Science, 1999, 9(1): 33.
5 Zhang, Z. et al. Hyperbolic heat propagation in a spherical solid medium under extremely high heating rates. In: AIAA/ASME Joint Thermophysics and Heat Transfer Conferences, 1998, 3: 275.
6 Glass, D. et al. Hyperbolic heat conduction with surface radiation. Int. J. Heat Mass Transfer, 1985, 28(10): 1823.
7 Joseph, D. et al. Heat waves. Rew. Mod. Phys., 1989, 61(1): 41.